Comparative Study of Novel Axial Flux Magnetically Geared and Conventional Axial Flux Permanent Magnet Machines

Mohammed F.H. Khatab, Z.Q. Zhu, *Fellow*, *IEEE*, H. Y. Li, and Y. Liu

Abstract - **In this paper, a performance comparison between the novel axial flux magnetically geared machines (AFMG) and the conventional axial flux YASA machine is presented. The AFMG and YASA machines have the same stator construction in which segments are equipped with concentrated windings to form the stator. However, the AFMG machine has two rotors with different pole-pair numbers. Magnetic gear effect can be obtained to increase the torque density. The performance comparisons at no-load and on-load conditions are then studied by 3D-finite element analysis (FEM). Moreover, both machines are prototyped, tested and compared.**

Index Terms—**Axial flux magnetically geared machine, finite element analysis, performance comparison, YASA machine**

I. Introduction

Axial flux permanent magnet (AFPM) machines have prominent advantages over radial flux PM (RFPM) machines since they have the merits of high torque density, low rotor losses, and high efficiency [1]. AFPM machines can be classified to two main configurations; double stator/single rotor (internal rotor) and double rotor/single stator (internal stator). Internal stator AFPM machines have been developed for high performance applications. Among the internal stator AFPM machines, the yokeless and segmented armature (YASA) machine has a unique design which is distinguished by a modular stator construction and has shown to exhibit superior performance due to short end windings, high windings filling factor and reduced stator core [2],[3].

In many indirect drive electromechanical systems, mechanical gearboxes are mostly coupled in series with PM machines in which regular maintenance and vibrations are the main drawbacks of such mechanical device. However, magnetic gears (MGs) have recently been proposed to replace conventional mechanical gears. MGs have competitive torque transmission capability compared with their mechanical counterpart [4]. Moreover, by integrating an MG into a conventional PM machine, a magnetically geared machine has been investigated and developed. It always has the merits of high torque density and reduced overall size in comparison with conventional PM machine axially combined with an MG [5]. Recently, axial flux magnetically geared (AFMG) machines have also been proposed for various applications which were firstly presented in [6]. Additionally, several axial flux magnetically geared machines topologies have been proposed for wind power generation applications [7-9], and hybrid electric vehicles (HEVs) [10].

Based on YASA machine, a novel AFMG machine has been presented in [11] and for power split applications in HEVs has been proposed in [12]. The presented machine essentially has the same stator structure of the conventional YASA machine. However, since YASA machine comprises of two identical PM rotors, the new AFMG machine was created by different rotor pole pairs for two rotors.

In this study, the proposed AFMG machine and the YASA machine with the same volume will be comparatively studied. Moreover, the machine performance at no-load and on-load will be compared. Furthermore, measured results of both machine prototypes will be compared.

II. Machine Geometries and Principle of Operation

The configurations of the YASA machine and the proposed AFMG machine are shown in Fig. 1. The YASA machine has a stator which is formed by separated iron segments equipped with concentrated windings, and is sandwiched between two identical surface mounted PM rotors physically connected to each other, Fig. 1(a). On the other hand, the proposed AFMG machine has the same stator construction of the YASA machine, the only difference being the two surface mounted PM rotors with different pole pairs. One rotor rotates at lower speed named as LSR and the other at higher speed named as HSR, Fig. 1(b). Since the proposed magnetically geared machine designated as MG12/10-14 has a 12 stator pole and two different rotors of 10 pole HSR and a 14 pole LSR, two YASA machine topologies with a 12 pole stator are considered for this study. The first YASA machine topology designated as YASA12/10 has a 10 pole rotor and the second topology designated as YASA12/14 has a 14 pole rotor. With the same machine volume, axial length and copper loss, the AFMG machine and YASA machine topologies have been optimised for maximum torque by utilizing 3D-FEA. The specifications, optimal dimensions and materials of two machines are listed in Table I.

For a conventional YASA machine, the total machine electromagnetic torque is the summation of both individual rotor torques produced by the interaction between the armature reaction flux and PM flux. However, since the proposed machine is a combination of an MG and a PM machine, its operation principle is based on these two

Manuscript was submitted for review on 23, July, 2018.

Mohammed F.H. Khatab is currently pursuing the Ph.D. degree in electrical engineering at University of Sheffield, Sheffield, UK. (e-mail: mfhkhatab1@sheffield.ac.uk)

Z.Q. Zhu is with the University of Sheffield. (e-mail: z.q.zhu@sheffield.ac.uk).

H. Y. Li is currently pursuing the Ph. D. degree at University of Sheffield.(e-mail: hli53@sheffield.ac.uk)

Y. Liu is currently working toward the Ph.D. degree in the Department of Electronic and Electrical Engineering, University of Sheffield (e-mail: YLiu147@sheffield.ac.uk).

Digital Object Identifier 10.30941/CESTEMS.2018.00050

machines. The operation principle of MGs has been explained in details in [4]. When one rotor is driven by specific torque at a specific speed, the magnetic flux produced by its PMs is modulated by the iron pieces located in between rotors which results in space harmonics on the other rotor's air-gap has the same pole-pairs and rotational speed. Assuming that the HSR has p_h pole pairs with angular speed of ω_h, and the LSR has p_l pole pairs with speed of ω_l, a high transferred torque is obtained when the relation between the numbers of pole pairs of HSR, LSR and the stationary pole pieces n_s is stated as [4].

$$p_l + p_h = n_s \tag{1}$$

In addition, with stationary stator pieces, the gear ratio G_r, can be expressed by

$$G_r = -\frac{p_l}{p_h} = \frac{\omega_h}{\omega_l} = \frac{T_l}{T_h} \tag{2}$$

where, T_l and T_h are the torques of LSR and HSR respectively.

When one rotor is connected to the prime-mover at specific speed, the torque/speed are scaled up/down to the other rotor due to the MG effect. The negative sign indicates that two rotors rotate at opposite directions.

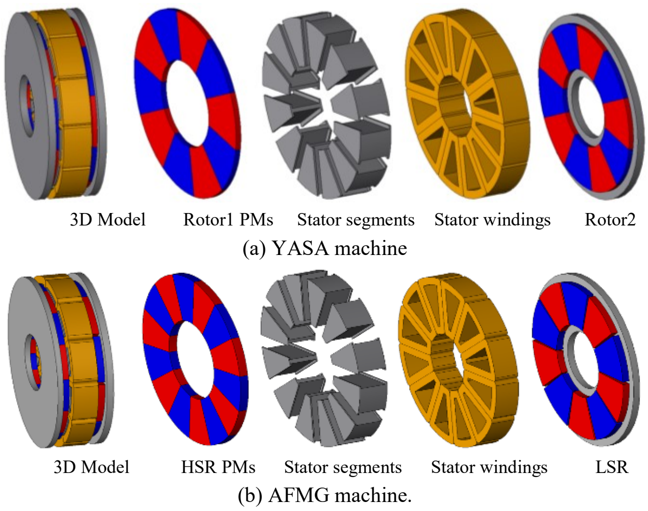

Fig. 1. The proposed machine topology.

TABLE I
PARAMETERS OF THE MACHINES.

Parameter	MG 12/10-14	YASA 12/10	YASA 12/14
High speed (r/min)	400	400	-
Low speed (r/min)	285.5	-	285.5
HSR pole No. (P_h)	10	10	-
LSR pole No. (P_l)	14	-	14
Stator pole number (n_s)	12	12	12
Machine inner diameter (mm)	30	30	30
Machine outer diameter (mm)	90	90	90
Axial length (mm)	25	25	25
Air gap length (mm)	0.5	0.5	0.5
Number of turns /phase	80	80	80
Packing factor	0.5	0.5	0.5
Armature stator axial length (mm)	12	13.6	14
Rotor axial length (mm)	6	5.17	5
Rated current RMS (A)	13.5	14.5	14.8
PM remanence B_r (T)		1.2	
PM permeability (μ_r)		1.05	
PM resistivity (Ωm)		1.4×10^{-5}	
PM volume (cm^3)	26263.6	16587.6	16691.2

In addition, concentrated windings are employed for the proposed AFMG machine. Various combinations of slot and pole numbers result in different winding layouts. Therefore, in addition to the torque exerted at both rotors due to the MG effect, the armature reaction windings can produce flux in both air-gaps. The torque produced by the interaction between the armature reaction flux harmonics and PMs flux harmonics for each rotor will be added to the MG torque of each rotor. Moreover, the torque produced by armature reaction can be controlled by the current angle. Consequently, this torque can be added to either HSR or LSR which can be decided according to the considered output rotor.

III. PERFORMANCE COMPARISON OF AFMG MACHINE WITH CONVENTIONAL YASA MACHINE

With the aid of 3D-FE analysis, the 3-phase AFMG machine and the 3-phase YASA machine are analysed and compared. By considering both no-load condition, in which the winding current is zero, and on-load condition, in which the winding is applied by specific current, a performance comparison between the proposed AFMG machine and YASA machine topologies is performed. For the AFMG machine, two no-load conditions are taken into consideration in this study. The first condition when the relative angle between HSR and LSR pole axes is zero electrical degree, in which the MG effect torque is being canceled. Moreover, with the aim of obtaining maximum MG effect torque, both rotors are located at a relative angle between such rotor pole axes of 90 electrical degree [13]. Furthermore, since the AFMG machine has two rotors with two different poles and speeds, either HSR or LSR can be considered as an output rotor which is connected to the drive load. Therefore, the MG12/10-14 machine performance is compared with the YASA12/10 machine when the 10 pole HSR is assumed as an output rotor in which the LSR of 14 poles is connected to the prime-mover. Similarly, the machine is compared with the YASA12/14 machine when the 14 pole LSR is assumed as an output rotor.

A. Flux linkage and back EMF

A comparison of the no-load results of the proposed MG12/10-14 and YASA machines is firstly obtained. It should be mentioned that to calculate the flux linkage and back EMF of the AFMG machine, the initial relative angle between both rotors is adjusted at zero electrical degree. Moreover, since the proposed machine has two rotors with two different speeds as stated in (2), the back EMF of the YASA machine is presented at the same speeds of the AFMG machine rotors. On the other hand, the back EMF of the YASA12/14 machine will be presented at the same speed of LSR (285.7 r/min) and similarly for the YASA12/10 machine at the same speed of HSR (400 r/min).

Fig. 2 shows the phase flux linkages of the MG12/10-14 machine compared with the YASA12/10 and YASA12/14 machines at rated speeds. It is clear that the flux linkage of the YASA12/10 machine has the highest amplitude value of proximately 18.4 mWb. Whereas, the MG12/10-14 and YASA12/14 machines have amplitude values of 17.2 and 14.8 mWb, respectively. The YASA12/14 machine has smaller rotor pole pitch compared with the stator pole pitch results in lower flux passing to the stator pole. However, since the proposed machine has a combination of two YASA topologies in which both rotors contribute to the total flux linking the stator windings, the flux linkage amplitude is between both YASA machine flux linkage amplitudes.

In addition, the phase back EMFs and the coresponding harmonics are also compared and ploted in Fig. 3. It indicates that the amplitude of the phase back EMF is approximatly 3.80 V for the YASA12/10 machine at 400 r/min. Moreovre, a maximum back EMF of aproximatlly 3.0 V can be gained by the YASA12/14 machine at 285.7 r/min. Furthermore, for the MG12/10-14 machine, both HSR and LSR PMs contribute to the total back EMF in which at a 400 r/min HSR speed and a 285.7 r/min LSR speed, the amplitude of the phase back EMF is aproximatly 3.67 V.

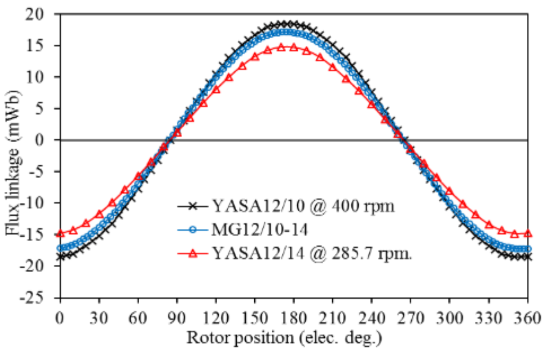

Fig. 2. Comparison of no-load flux linkage waveforms at rated speeds.

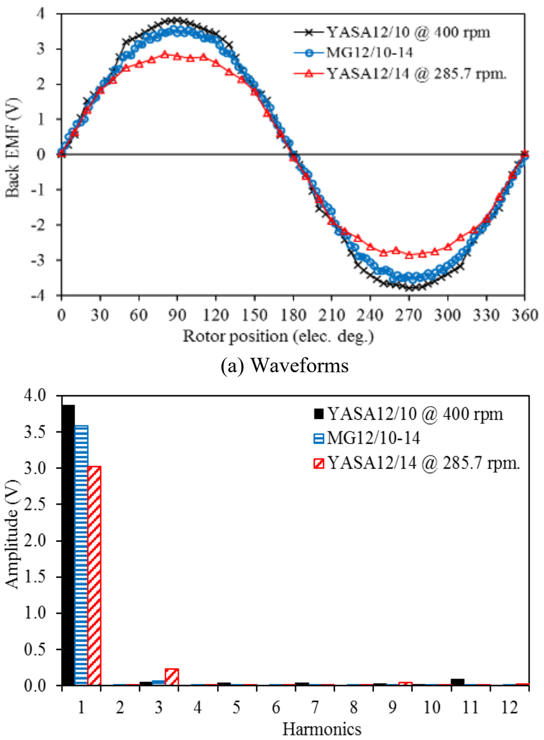

(a) Waveforms

(b) Harmonic spectra

Fig. 3. Comparison of no-load phase back EMF waveforms at rated speeds.

B. Cogging torque

A comparison of cogging torques of the proposed MG12/5-7 and YASA machines is performed. For the AFMG machine simulation, the initial positions for HSR and LSR are adjusted at zero. Moreover, for comparison purpose, the cogging torque for one rotor of the YASA machines is individually examined using FEA which allows the calculation of the cogging torque of each rotor separately. The cogging torques of the HSR of AFMG and YASA12/10 machines are compared in Fig. 4. It is clear that the proposed machine HSR cogging torque has the lowest amplitude of 0.03 Nm while amplitudes of the total and individual rotor cogging torques are approximately 0.16 Nm and 0.08 Nm, respectively. Moreover, Fig. 5 compares the LSR and YASA12/14 cogging torques. As shown, the LSR also has a small cogging torque amplitude of 0.06 Nm compared to the YASA12/14 total and individual cogging torques of 0.24 Nm and 0.12 Nm, respectively.

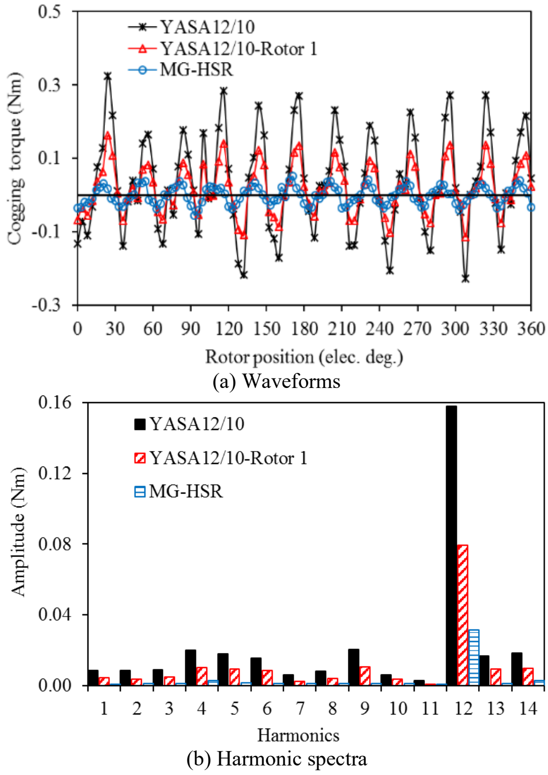

(a) Waveforms

(b) Harmonic spectra

Fig. 4. Comparison of HSR and YASA12/10 cogging torques.

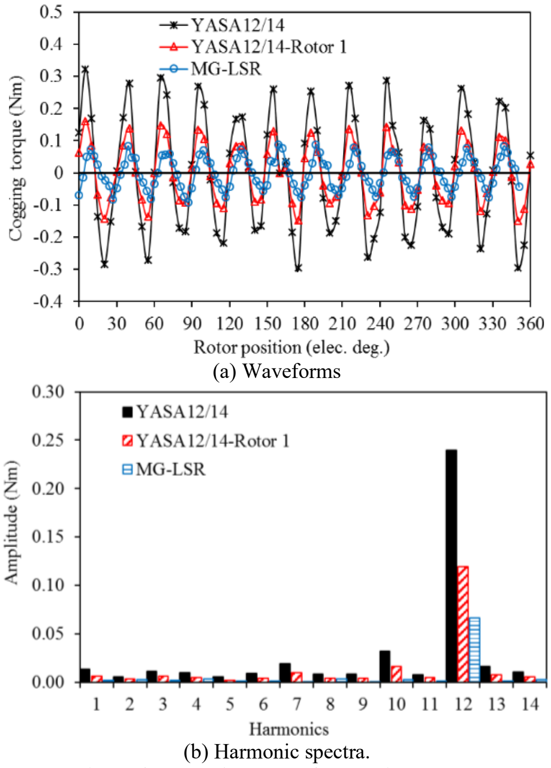

(a) Waveforms

(b) Harmonic spectra.

Fig. 5. Comparison of LSR and YASA12/14 cogging torques.

C. Torque

Fig. 6 shows a comparison between the LSR torque at no-load and on-load of the MG12/10-14 machine and the electromagnetic torque of the YASA12/14 machine. It should be mentioned that the no-load torque of AFMG machine is calculated at initial relative angle position of 90 electrical degree. It can be seen that when the LSR is considered as an output rotor, the no-load LSR average torque is significantly higher than the on-load average torque of the YASA12/14 machine of 5.30 Nm and 3.2 Nm. respectively. Moreover, the LSR average torque increases further to reach just below 7 Nm when rated current is applied to the machine windings. Similarly, when HSR is considered as an output rotor, a comparison of HSR and YASA12/10 average torques is illustrated in Fig. 7. It can be evidenced that maximum average torques of approximately 3.8 Nm and 5.1 Nm can be obtained by HSR at no-load and on-load conditions, respectively. Both torques are also higher than the YASA12/10 machine torque at rated current of approximately 2.8 Nm.

Furthermore, since the machines have the same size, the torque density is significantly improved when the MG is combined with the AFPM machine. When the LSR is considered as an output rotor, a maximum torque density of approximately 33 kNm/m^3 and 43 kNm/m^3 can be obtained by the AFMG machine at no-load and on-load conditions, respectively. In contrast, a torque density of approximately 20 kNm/m^3 can be achieved by the YASA12/14 machine at on-load condition. Correspondingly, when HSR is assumed as an output rotor, the torque densities of the AFMG machine at no-load and on-load conditions are approximately 24 kNm/m^3 and 32 kNm/m^3, respectively. In contrast, a torque density of approximately 17 kNm/m^3 is obtained by the YASA12/10 machine at on-load condition. It can be concluded that the MG effect due to the mechanical input power significantly increases the torque density. On the other hand, with the benefit of two rotors with different speeds, the torque obtained by armature current is improved by the torque attributed by MG effect.

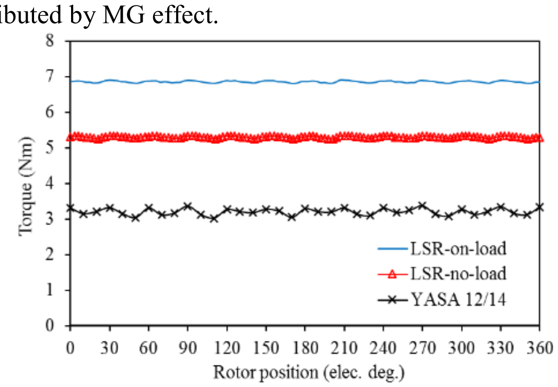

Fig. 6. Comparison of LSR and YASA12/14 torques.

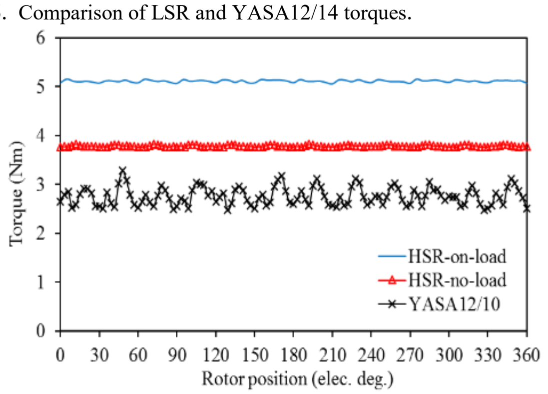

Fig. 7. Comparison of HSR and YASA12/10 torques.

D. Losses and efficiency

With the aid of 3D-FEA, iron loss and PM eddy current loss are calculated for the machines. Since the MG12/10-14 machine has two rotors with different speeds, the iron losses of the YASA12/10 machine is calculated at the same speed with HSR (400 r/min). The losses of the YASA12/14 machine is calculated at the same speed with LSR (285.7 r/min). The iron and PM eddy current losses in AFMG and YASA machines at rated speeds under no-load condition are compared in Fig. 8. The comparison indicates that the MG12/10-14 machine has higher iron loss and total loss than the other two machines. The YASA12/10 machine has the highest PM loss among all the machines whereas the YASA12/14 machine has the lowest PM loss as a result of low speed of rotation. Moreover, Fig. 9 compares the on-load iron and PM eddy current losses as well as the corresponding efficiency at 30W copper loss for all the machines. Overall, for all the machines, the iron and PM eddy current losses slightly increase compared with those under no-load condition. It is clear that in spite of a relatively higher iron loss, the MG12/10-14 machine has a superior efficiency of approximately 86 % due to higher output torque compared to the other topologies. In contrast, the YASA12/14 machine has the lowest efficiency of 75 % since its rated speed and corresponding output power are low.

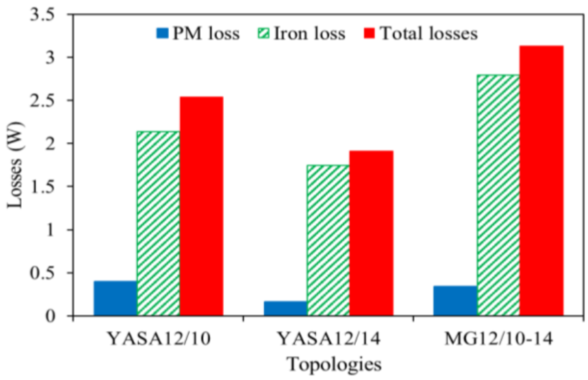

Fig. 8. Comparison of no-load losses of the proposed AFMG topology with YASA machine topologies.

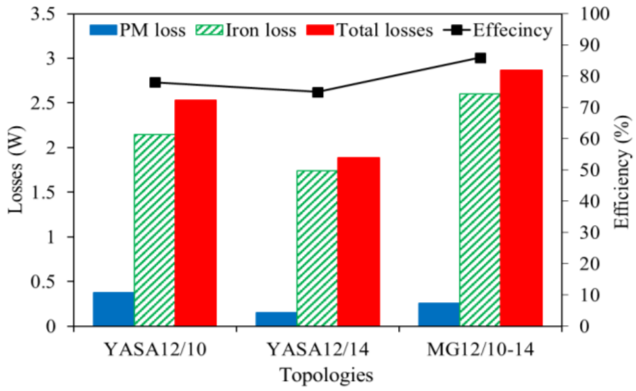

Fig. 9. Comparison of on-load losses and efficiency of the proposed AFMG topology with YASA machine topologies.

IV. Prototype Machines and Comparison of Experimental Results

Prototype machines of the proposed 3-phase magnetically geared machine and YASA machine were designed and built. The prototypes were so designed that the YASA machine can be employed by utilizing two identical 10-pole rotors physically connected to each other. However, by replacing one rotor of the YASA prototype with a 14-pole rotor, the prototype can realise the function of magnetically geared machine. The two prototypes are tested and compared at no-load and on-load. The prototype machine components are shown in Fig. 10 and the parameters are listed in Table II.

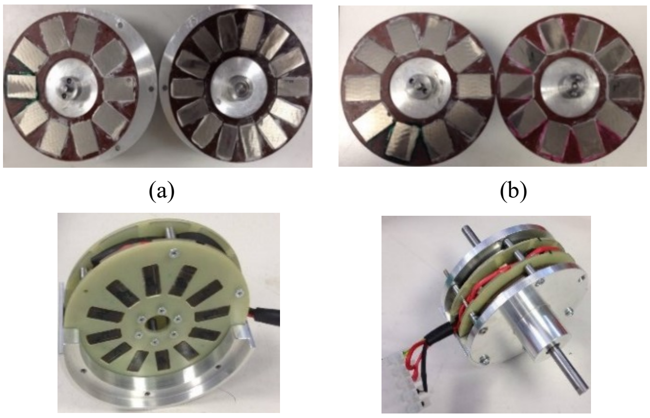

(a) (b)

(c) (d)

Fig. 10. Prototype machines. (a) HSR and LSR of AFMG. (b) YASA rotors. (c) Stator. (d) Assembled prototype.

TABLE II
PARAMETERS OF PROTOTYPE MACHINES

Parameter	MG 12/10-14	YASA 12/10
Rotor1 pole No. (P_h)	10	10
Rotor2 pole No. (P_l)	14	10
Stator pole No. (S_t)	12	
Stator inner diameter (mm)	48	
Stator outer diameter (mm)	88	
Stator axial length (mm)	16	
Axial length (mm)	30	
Air gap length (mm)	0.5	
Number of turns /phase	168	
Winding resistance /phase (Ω)	0.5	
Winding inductance /phase (mH)	0.54	
Rotor1 pole dimensions (mm)	(14×20)	
Rotor2 pole dimensions (mm)	(10×20)	(14×20)
Rotor1 PM thickness (mm)	3	3
Rotor2 PM thickness (mm)	3.5	3
Magnet remanence B_r (T)	1.21	
PM volume (cm^3)	1820	1680
Rated current Max. (A)	6	6

A. No-load Back EMF

The no-load phase back EMFs of magnetically geared machine and YASA machine prototypes were performed and validated with the 3D-FE results. To do that, the YASA prototype and the HSR of the AFMG prototype are driven by a prime-mover at 400 r/min. Fig. 11 shows a comparison of predicted and measured back EMFs of the YASA machine together with the AFMG machine. It can be evidenced that the phase back EMF amplitude of the YASA machine is slightly higher for the predicted and measured values, being approximately 7V and 6.7V, respectively, whereas the AFMG machine has the predicted and measured back EMF amplitudes of approximately 6.2V and 5.9V, respectively. In general, a good measured result validations are achieved for both prototypes.

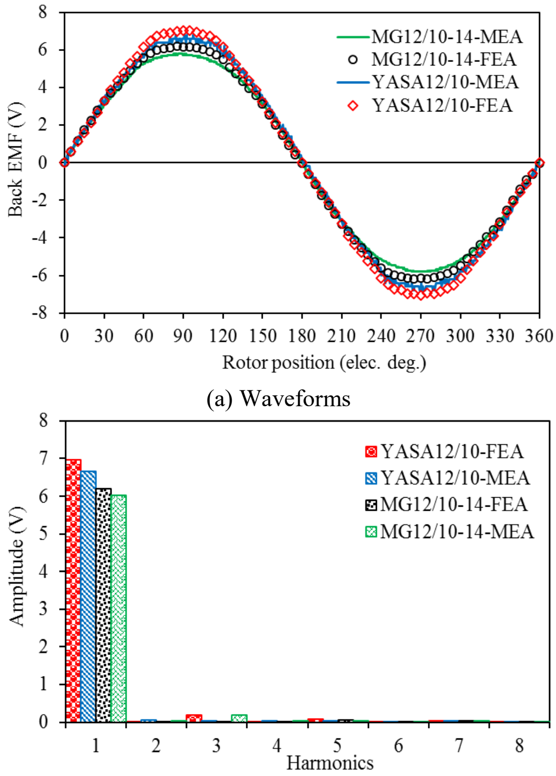

(a) Waveforms

(b) Harmonic spectra

Fig. 11. Comparison of measured and predicted Back EMFs of AFMG and YASA12/10.

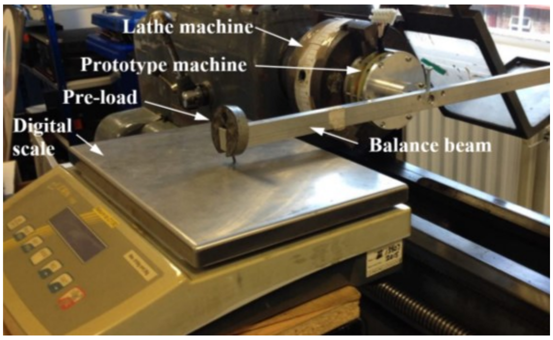

Fig. 12. Prototype machines test rig.

B. Static torque

With the aim of performing the static torque test for both prototypes, the measuring method described in [14] was employed with the aid of the test rig indicated in Fig. 12. For the YASA machine, the machine shaft is connected to a balanced beam and the force is calculated by a digital weight scale. The stator is connected to a lathe machine and rotated to change the rotor position. However, for the proposed magnetically geared machine, one rotor was fixed in place to the stator by a clamp which was fixed to the lathe machine. The fixed rotor pole axis is aligned to phase (A) pole axis. The other rotor is connected to the balanced beam in which the force produced by such rotor can be calculated by the digital weight scale. Moreover, a DC current is supplied to the phase windings (I_A, I_B, I_C) in which (I_A= – 2I_B= – 2I_C). Fig. 13 shows a comparison of the static torque and torque – current relationship for the YASA machine and the LSR at half-load and full-load whereby the LSR of magnetically geared machine is assumed as the output torque. Similarly, Fig.14 shows a comparison of the YASA machine static torque and torque-current curves with the HSR of the AFMG machine. It is evident that for both prototype machines, the measured and predicted results are in good agreement. However, maximum torque of HSR and LSR are significantly higher than the conventional YASA machine maximum torque. The MG effect noticeably increases the torque density since the resulting torque of the magnetically geared machine is the summation of armature reaction and MG effect torques.

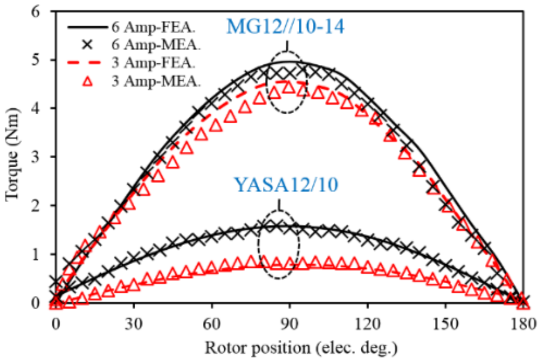

(a) Static torque

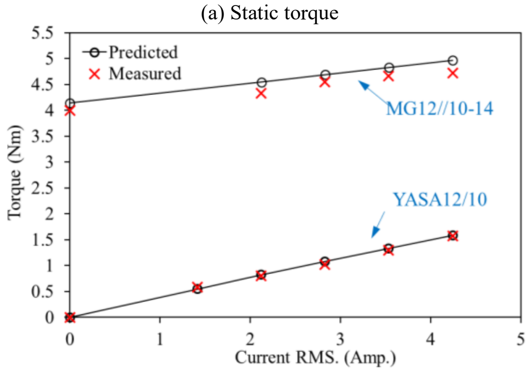

(b) Torque – current curves

Fig. 13. Comparison of measured and predicted LSR and YASA12/10 torques.

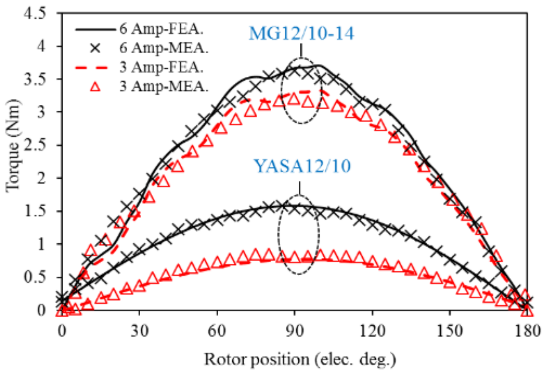

(a) Static torque.

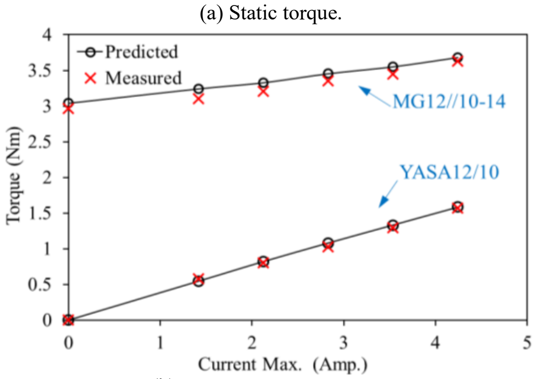

(b) Torque – current curves.

Fig.14. Comparison of measured and predicted HSR and YASA12/10 torques.

V. Conclusion

In this study, the no-load and on-load performances of the proposed axial flux magnetically geared machines and the conventional YASA machine have been analysed and compared. Simulation results show that a significantly higher torque density can be obtained by the proposed machine compared with the YASA machine. Moreover, both machines have been prototyped and the experiment results have been performed and compared. The measured results stated that the YASA machine has slightly superior performance at no load whereas the AFMG machine has significantly higher torque compared with the conventional AFPM machine.

References

[1] M. Aydin, H. Surong, and T. A. Lipo, "Torque quality and comparison of internal and external rotor axial flux surface-magnet disc machines", *IEEE Trans. on Ind. Elect.*, , vol. 53, no.3, pp. 822-830, June 2006.

[2] T. J. Woolmer and M. D. McCulloch, "Analysis of the yokeless and segmented armature machine," *in Proc. IEEE Int. Elec. Mach. Drives Conf.*, 2007., pp. 704-708.

[3] W. Fei, P. Luk, and K. Jinupun, "A new axial flux permanent magnet segmented-armature-torus machine for in-wheel direct drive applications," *IEEE Power Elect. Spec. Conf., 2008*, pp. 2197-2202, 15-19 June 2008.

[4] K. Atallah and D. Howe, "A novel high-performance magnetic gear," *IEEE Trans. on Magn.*, vol. 37, no.4, pp. 2844-2846, Jul. 2001.

[5] L. L. Wang, J. X. Shen, P. C. K. Luk, W. Z. Fei, C. F. Wang, and H. Hao, "Development of a magnetic-geared permanent-magnet brushless motor," *IEEE Trans. on Magn.*, vol. 45, no.10, pp. 4578-4581, Oct. 2009.

[6] N. Niguchi, K. Hirata, A. Zaini, and S. Nagai, "Proposal of an axial-type magnetic-geared motor," *in Proc, 20th Int. Conf. Elect. Mach.*, 2012, pp. 738-743.

[7] R. J. Wang, L. Bronn, S. Gerber, and P. M. Tlali, "Design and evaluation of a disc-type magnetically geared PM wind generator," *in 4th Int. Conf. Power Eng., Energy and Elect. Drives*, pp. 1259-1264.May 2013.

[8] M. Johnson, M. C. Gardner, and H. A. Toliyat, "Design and analysis of an axial flux magnetically geared generator," *IEEE Energy Conv. Congr. Expo.* , 2015, pp. 6511-6518.

[9] S. Niu, Y. Liu, S. L. Ho, and W. N. Fu, "Development of a novel brushless power split transmission system for wind power generation application," *IEEE Trans. on Magn.*, vol. 50, no. 11, pp. 1-4, Nov.2014.

[10] C. Tong, Z. Song, P. Zheng, J. Bai, and Q. Zhao, "Research on electromagnetic performance of an axial magnetic-field-modulated brushless double-rotor machine for hybrid electric vehicles," *in Proc. 17th Int. Conf. Elec. Mach. Sys.*, 2014, pp. 2896-2902.

[11] M. F. H. Khatab, Z. Q. Zhu, H. Y. Li, and Y. Liu, "Optimal design of a novel axial flux magnetically geared PM machine", *Twelfth Inter. Conf. on Ecolo.Vehi. and Renewable Energies (EVER)*, 2017, pp. 1-8.

[12] Z. Q. Zhu, M. F. H. Khatab, H. Y. Li, and Y. Liu, "A novel axial flux magnetically geared machine for power split application", *Twelfth Int.Conf. Ecolo. Vehicles and Renewable Energies (EVER)*, 2017, pp. 1-8.

[13] N. W. Frank and H. A. Toliyat, "Gearing ratios of a magnetic gear for wind turbines," *in Proc. IEEE int. Elec. Mach. Drives Conf.*, 2009, pp. 1224-1230.

[14] Z. Q. Zhu. "A simple method for measuring cogging torque in permanent magnet machines". *in Proc. IEEE . power & Energy Society General Meeting (PES)*, Calgary, 26–30 July 2009; pp. 1–4.

Mohammed F. Khatab received the B.S. degree from Omar-Almukhtar (OMU) University, El Bayda, Libya, in 1999 and the M.S. degree from University of Newcastle, Newcastle upon Tyne, UK, in 2010, all in electrical and electronic engineering. He is currently pursuing the Ph.D. degree in electrical engineering at University of Sheffield, Sheffield, UK. His research interest includes design and control of permanent magnet and magnetic geared machines.

Z. Q. Zhu (M'90–SM'00–F'09) received the B.Eng. and M.Sc. degrees from Zhejiang University, Hangzhou, China, in 1982 and 1984, respectively, and the Ph.D. degree from The University of Sheffield, Sheffield, U.K., in 1991, all in electrical and electronic engineering.

Since 1988, he has been at The University of Sheffield, where he currently holds the Royal Academy of Engineering/Siemens Research Chair and is the Head of the Electrical Machines and Drives Research Group, the Academic Director of Sheffield Siemens Wind Power Research Centre, the Director of Sheffield CRRC Electric Drives Technology Research Centre, and the Director of Midea Electrical Machines and Controls Research Centre. His research interests include the design and control of permanent-magnet machines and drives for applications ranging from automotive through domestic appliances to renewable energy.

Prof. Zhu is a Fellow of Royal Academy of Engineering.

Hua-Yang Li was born in Shanxi, China, in 1992. He received the B.Eng. and M.Sc. degrees in electrical engineering from Zhejiang University, Hangzhou, China, in 2013 and 2016. He is currently pursuing the Ph. D. degree at University of Sheffield, Sheffield, U.K. His research interests include design of magnetic gears and permanent magnet machines.

Yue Liu (S'16) received the B.Eng. and M.Sc. degrees in electrical and electronic engineering from Harbin Institute of Technology, Harbin, China, in 2013 and 2015, respectively. He is currently working toward the Ph.D. degree in the Department of Electronic and Electrical Engineering, University of Sheffield, Sheffield, U.K.